DENSITY AND TEMPERATURE DIAGNOSTICS OF SOLAR EMISSION LINES FROM Ne VI AND Mg VI

P. K. RAJU
Indian Institute of Astrophysics, Bangalore-560034, India

and

ASHEESH K. GUPTA
Department of Applied Physics, Institute of Technology, Banaras Hindu University, Varanasi 221005, India

(Received 6 August, 1990; in revised form 13 November, 1992)

Abstract. Line intensity ratios of Ne VI lines with respect to a resonance line of Mg VI have been considered for electron density and temperature determinations within the chromosphere–corona transition region. The electron pressure within the transition region has been assumed to be constant. In addition, these ratios would enable us to estimate the relative element abundances of neon to magnesium. An attempt has been made to explain the extreme ultraviolet intensities of Ne VI and Mg VI lines as observed by ATM ultraviolet spectrometer. The observed intensities correspond to the average quiet-Sun conditions near solar minimum. Theoretical intensities for Ne VI and Mg VI lines have been computed using a model solar atmosphere. Theoretical intensities obtained by using the values 3.98×10^{-5} and 3.16×10^{-5} for element abundance of Ne and Mg, respectively, seem to agree well with the expected intensities. The agreement between some of the expected and computed intensities suggests the need for future observations at higher spectral resolutions to resolve difficulties arising out of blending due to two or more lines.

1. Introduction

Electron density and temperature diagnostics of solar plasma using emission lines have been extensively reviewed (Gabriel and Jordan, 1972; Dwivedi, 1988). The usual procedure has been to look for intensity ratios which are sensitive either to electron density (n_e) or electron temperature (T). In various investigations it has been noticed that the quiet-Sun electron pressure ($n_e T$) within the chromosphere–corona transition region seems to have a constant canonical value of 6×10^{14} cm^{-3} K (Doschek, 1984). The observed intensity of a particular Ne VI or Mg VI line is due to the several emitting layers. Each layer would have different electron density and temperature values but the electron pressure would be same in each of the emitting layer. It is, therefore, physically meaningful to study the variation of theoretical intensity ratios with electron density (and thus temperature) at constant electron pressure. The comparison of theoretical ratios with observed ratios would then give effective values of electron density and temperature within the emission regions. The ions Ne VI and Mg VI have their respective maximum relative ion abundance at the same temperature (Jordan, 1969) and their ionization equilibrium curves overlap around this temperature. Therefore, Ne VI and Mg VI ions would be rather useful for the density and temperature diagnostics of the transition region.

Vernazza and Reeves (1978) have published a detailed paper on extreme ultraviolet

Solar Physics **145:** 241–256, 1993.

composite spectra of representative solar features. The composite spectra are from the ATM ultraviolet spectrometer data with a spectral resolution of 1.6 Å over the range 280–1350 Å. The absolute intensities, as listed by them, for Ne VI and Mg VI lines relevant to the average quite-Sun conditions form the basis of the present investigation.

The ion Ne VI has two fine structure levels in the ground state. The relative populations of these fine structure levels are constant for electron densities and temperatures relevant for the formation of Ne VI lines. Using this information and the observed intensity of the Ne VI resonance line at 562.8 Å we have analysed and discussed the intensities of the other Ne VI lines. We have calculated theoretical intensities for several Ne VI and Mg VI lines using a model solar atmosphere. The theoretical intensities agree rather well with the expected intensities when we choose element abundance values of 3.98×10^{-5} and 3.16×10^{-5} for Ne and Mg, respectively.

In Section 2, we briefly describe line emissivity. Atomic data used are discussed in Section 3. Observed and theoretical line intensities are discussed in Section 4. Electron density and temperature diagnostic aspects of line intensity ratios are examined in Section 5.

2. Line Emissivity

The volume emission coefficient in a radiative transition from the upper level j to a lower level i is given by

$$\varepsilon(ij) = N_j A(ji) \frac{\hbar c}{4\pi\lambda_{ij}} \text{ erg cm}^{-3}\text{ s}^{-1}\text{ sr}^{-1} . \tag{1}$$

The wavelength for the transition is λ_{ij}, $\hbar$ is Planck's constant, c is the velocity of light, and $A(ji)$ is the spontaneous transition probability. The number density N_j of the emitting level can be further expressed as

$$N_j(X^{+m}) = \frac{N_j(X^{+m})}{N(X^{+m})} \frac{N(X^{+m})}{N(\mathrm{X})} \frac{N(\mathrm{X})}{N(\mathrm{H})} \frac{N(\mathrm{H})}{n_e} n_e , \tag{2}$$

where X^{+m} denotes the mth ionization stage of the element X, $N_j(X^{+m})/N(X^{+m})$ is the population of level j relative to the total population of the ion X^{+m}, $N(X^{+m})/N(\mathrm{X})$ is the ionization ratio of the ion X^{+m}. $N(\mathrm{X})/N(\mathrm{H})$ is the abundance of the element X relative to hydrogen. We have assumed $N(\mathrm{H})/n_e = 0.8$ for the fully-ionized plasma. The emissivity can now be written as

$$\varepsilon_{(ij)} = \frac{1.59 \times 10^{-8}}{4\pi\lambda_{ij}\,(\text{Å})} A(ji) \frac{N_j(X^{+m})}{N(X^{+m})} \frac{N(X^{+m})}{N(\mathrm{X})} \frac{N(\mathrm{X})}{N(\mathrm{H})} n_e . \tag{3}$$

We denote the observed line emission as $I(\lambda_{ij})$. This is the intensity integrated over the line of sight. In the case of two lines emitted from the same ion, the intensity ratio can be expressed as

$$\frac{I(\lambda_{ij})}{I(\lambda_{kl})} = \frac{A(ji)}{A_{(lk)}} \frac{\lambda_{kl}}{\lambda_{ij}} \frac{N_j(X^{+m})}{N_l(X^{+m})} . \tag{4}$$

The intensity ratio for the lines emitted from the same volume element but from different elements X and Y is then given by

$$\frac{I(\lambda_{ij})}{I(\lambda_{kl})} = \frac{A(ji)}{A(lk)} \frac{\lambda_{kl}}{\lambda_{ij}} \, p(j, l, x, y) q(x, y) N(x, y) , \tag{5}$$

where

$$p(j, l, x, y) = \frac{N_j(X^{+m})}{N(\mathrm{X})} \bigg/ \frac{N_l(Y^{+n})}{N(\mathrm{Y})} ,$$

$$q(x, y) = \frac{N(X^{+m})}{N(\mathrm{X})} \bigg/ \frac{N(Y^{+n})}{N(\mathrm{Y})} ,$$

$$N(x, y) = \frac{N(\mathrm{X})}{N(\mathrm{H})} \bigg/ \frac{N(\mathrm{Y})}{N(\mathrm{H})} .$$

In the second case the intensity ratio depends on the relative ionic concentrations of the element and the relative element abundances. The ionization equilibrium curves of Ne VI and Mg VI almost overlap around the temperature for maximum ion concentration. We, therefore, assume that lines from these two ions originate from the same emitting layers. This assumption then justifies the use of the Equation (5) for line intensity ratios. We have solved the steady state equations for the various levels to obtain N_j(Ne VI)/N(Ne VI) and N_l(Mg VI)/N(Mg VI) as a function of electron density and temperature. Electron density and temperature values are restricted by the constant electron pressure parameter ($n_e T$). The first 11 lowermost levels are assumed for Ne VI. For Mg VI the first 13 levels are considered.

3. Atomic Data

The atomic data needed to compute line intensities are the following: (i) wavelengths, (ii) the radiative transition probabilities, and (iii) collision strengths. The wavelengths for Ne VI lines have been taken from Kelly and Palumbo (1973). Mg VI line wavelengths are from Edlen (1984).

Radiative probabilities

Mg VI ion: the spontaneous radiative probabilities for allowed transitions have been obtained in the following manner: For a given transition radiative probabilities of Ne IV (Bhatia and Kastner, 1988), Mg VI, Si VIII, S X, Ar XII, Ca XIV (Bhatia and Mason, 1980) were plotted against inverse of atomic number. A smooth curve was obtained through the various points. The graphical values were then used in the actual computations. In the case of the transition at 387.97 Å, Wiese, Smith, and Miles (1969) value was used. Similar procedure was adopted for the transitions between the doublet ground term levels and the excited ^4P levels. Spontaneous radiative probabilities for transitions among the ground state fine structure levels have been taken from Zeippen (1982).

Ne VI *ion*: in the case of Ne VI transitions we have used the spontaneous transition probabilities of O IV, Na VII, Si X, and S XII (Flower and Nussbaumer, 1975a, b). The procedure is the same as that for the Mg VI ion. Radiative excitation rate among the two fine structure levels of the ground term of Ne VI has been estimated by assuming radiation temperature of 5000 K and a dilution factor of $\frac{1}{2}$. We have also considered the stimualted emission rate for transitions between the two fine structure levels.

COLLISION STRENGTHS (Ω_{ij})

Mg VI *ion*: for a particular optically allowed transition $\log(\Omega_{ij} Z^2)$ for Ne IV (Bhatia and Kastner, 1984), Mg VI, Si VIII, S X, Ar XII, and Ca XIV (Bhatia and Mason, 1980) were plotted against Z^{-1}. Z is the residual charge on the ion. The corresponding Ω_{ij} for Mg VI was then obtained from the graphical value on the smooth curve. A similar procedure was adopted for intersystem transitions and forbidden transitions involving upper excited levels. In the case of forbidden transitions Ω_{ij} values have been taken from Saraph, Seaton, and Shemming (1969) and Czyzak, Aller, and Euwema (1974). We noticed that $\log(\Omega_{ij} Z^2)$ vs Z^{-1} for a forbidden transition can be fitted with a straight line. Bhatia and Kastner (1984) suggest that Ω_{ij} (forbidden) values for Ne IV calculated by Giles (1981) should be preferred. We have estimated for Ne IV the difference, Δ, between $\log(\Omega_{ij} Z^2)$ values according to Giles (1981) and our linear fit. In view of the linear fit we have used the same Δ for Mg VI transitions and obtained the corrected Ω_{ij} (forbidden) values for use in our calculations. Revised forbidden Ω_{ij} values used by us are, for most of the transitions, larger by a factor of 1.5 to 2 than that of Bhatia and Mason (1980). Our Ω_{ij} value for the transition ${}^2D^0_{5/2} - {}^2D^0_{3/2}$ is larger by a factor of 3.3 to that of Bhatia and Mason (1980).

Ne VI *ion*: the collision strengths for all the transitions of O IV, Na VII, Si X, and S XII listed by Flower and Nussbaumer (1975a, b) have been plotted against the residual charge on the ion. The corresponding collision strengths for Ne VI transitions were then read off from the smooth curve.

4. Observed and Theoretical Intensities

Ne VI *lines*: the Ne VI ion has two fine structure levels in the ground state. The excited level populations are governed by the relative populations of the ground term levels. It is found that the relative population of the two fine structure levels is constant over the range of electron density and temperature relevant for the formation of Ne VI lines. The ratio of the upper level population of the ground term to that of the lower level works out to 2.04. Using this constant value and the observed intensity of the Ne VI resonance line at 562.80 Å we have attempted to infer the expected intensity of the other Ne VI lines and compare them with the observed values listed by Vernazza and Reeves (1978). The observed values considered correspond to the average quiet-Sun conditions at solar minimum.

The observed line at 561.4 Å has been identified as 562.8 Å Ne VI line along with 561.7 Å Ne VII line. The observed intensity is 18.31 ergs cm^{-2} s^{-1} sr^{-1}. Dufton, Doyle, and Kingston (1979) have shown that the contribution of Ne VII line to the total intensity is negligibly small. Therefore, we attribute the observed intensity to the two close Ne VI lines at 562.71 Å and 562.80 Å. It can be shown, using the constancy of the relative population of the two fine structure levels, that the 562.80 Å line would have an intensity of 16.65 ergs cm^{-2} s^{-1} sr^{-1}. The 562.71 Å line would then have an intensity of 1.66 ergs cm^{-2} s^{-1} sr^{-1}.

The 558.59 Å Ne VI line has a common upper level with the 562.71 Å line. The intensity of 558.59 Å line would then be given by the atomic data for the two transitions and the intensity of 562.7 Å line. This works out to 9.40 ergs cm^{-2} s^{-1} sr^{-1} for the 558.59 Å line. The observed line at 556.80 Å has been assigned by Vernazza and Reeves (1978) to 558.6 Å Ne VI line and 557.0 Å Ca X line. The observed intensity of 18.95 ergs cm^{-2} s^{-1} sr^{-1} is twice the expected value for the Ne VI line. We attribute the residual value of 9.55 ergs cm^{-2} s^{-1} sr^{-1} to Ca X line. This can be explained in the following way. The line at 573.0 Å has been assigned to 574.0 Å Ca X line by Vernazza and Reeves (1978) with an intensity of 7.81. The expected intensity of 574.0 Å Ca X line should be $\frac{1}{2}$ of 557.0 Å Ca X line. This amounts to 4.78 ergs cm^{-2} s^{-1} sr^{-1} for 574.0 Å Ca X line. We have attributed the residual intensity of 3.03 ergs cm^{-2} s^{-1} sr^{-1} to 574.28 Å C III line ($2s2p\ ^1P^0 - 2s3d\ ^1D$). This blending of C III line with Ca X line has not been mentioned by Vernazza and Reeves. We have arrived at this conclusion regarding C III line by considering collision strengths and other atomic data for the relevant transitions of C III and O V together with the observed 977.00 Å C III line intensity of 963.06 ergs cm^{-2} s^{-1} sr^{-1} (Vernazza and Reeves, 1978).

The observed line at 434.6 Å has been identified as 435.65 Å Ne VI line blending (probably) with the 434.9 Å Mg VII line. The expected observable intensity (based on the observed intensity of the 562.80 Å line) would be 7.10 ergs cm^{-2} s^{-1} sr^{-1}. The observed value is 28.32 ergs cm^{-2} s^{-1} sr^{-1}. The difference of 21.22 between the expected and observed intensity values has been attributed by us to 434.71 Å and 434.92 Å Mg VII lines. This is explained in the following way. It has been shown (Raju and Dwivedi, 1979) that for a spherically-symmetric solar atmosphere (Elzner, 1976) and for the element abundance value of 3.16×10^{-5} for Mg the computed intensities for 434.71 Å and 434.92 Å Mg VII lines are 2.27 and 13.39 ergs cm^{-2} s^{-1} sr^{-1}, respectively. In a similar manner assuming a value of 3.98×10^{-5} for Ne element abundance the computed intensity for 435.65 Å Ne VI line is 7.57 ergs cm^{-2} s^{-1} sr^{-1}. The agreement between the computed and expected Ne VI line intensities is very good. The combined computed intensities for Ne VI and Mg VII lines is 23.23. This value is quite close to the observed intensity at 434.6 Å.

The Ne VI line at 433.18 Å has an observable intensity of 4.26 ergs cm^{-2} s^{-1} sr^{-1} (based on the observed intensity at 562.80 Å). The computed value is 4.54. The absence of this line in the listing of Vernazza and Reeves (1978) is not clear. If we assume that this line blends with the observed line at 434.6 Å then the agreement between the combined computed intensities and the observed value becomes excellent. Future observations at high spectral resolutions are needed to resolve this difficulty.

The line at 403.1 Å has been identified as 403.2 Å Ne VI line blending (probably) with

403.3 Å Mg VI line. The observable intensity for this Ne VI line (based on the 562.80 Å line intensity) would be 4.55 ergs cm^{-2} s^{-1} sr^{-1}. The theoretical intensity works out to 4.83. The theoretical intensity for 403.31 Å Mg VI line is 13.01 ergs cm^{-2} s^{-1} sr^{-1}. Thus, the combined theoretical intensity is 17.84 ergs cm^{-2} s^{-1} sr^{-1}, a value close to the observed value of 25.73. The observed value is stated to have statistical error exceeding 10%. There could be some unknown blends which could reduce the discrepancy between the observed and the theoretical values.

The observed line at 401.3 Å has been assigned to 401.7 Å Ne VI line with an observed intensity of 89.00 ergs cm^{-2} s^{-1} sr^{-1}. The expected observable intensity for this line is 21.96. Theoretical value amounts to 23.40 ergs cm^{-2} s^{-1} sr^{-1}. Ne VI has a line at 401.14 Å close to the 401.70 Å line. The 401.14 Å line would have an observable intensity of 8.30 and a theoretical value of 8.85 ergs cm^{-2} s^{-1} sr^{-1}. These two lines might be blending with the Mg VI line at 400.66 Å with a theoretical intensity of 8.81 ergs cm^{-2} s^{-1} sr^{-1}. The combined theoretical intensity is smaller by a factor of 2.2 as compared to the observed value of 89.00. This discrepancy is not clear at present.

The observed line at 399.7 Å has been assigned probable identification status to Mg VI 399.2 Å line by Vernazza and Reeves. However, the Ne VI line at 399.82 Å would have an observable intensity of 4.41 ergs cm^{-2} s^{-1} sr^{-1} with a theoretical value of 4.69. Theoretical intensity for the Mg VI line would be 4.53. The combined theoretical intensity of 9.22 is smaller by a factor of 3 than the observed value of 30.06 ergs cm^{-2} s^{-1} sr^{-1}. The observed value has a statistical error exceeding 10%. The reason for the discrepancy between the observed and theoretical itnensities is not clear.

The weak Ne VI line at 999.6 Å would be blended with a strong Si XII 499.1 Å line in second order. Ne VI line would have an observable value of 0.91 ergs cm^{-2} s^{-1} sr^{-1} and a theoretical value of 1.00. The observed line at 1005.6 Å has been probably identified as Ne VI line at 1006.1 Å. The observed intensity is 5.02 ergs cm^{-2} s^{-1} sr^{-1}. The expected intensity (based on the 562.80 Å line intensity) is 0.55 and the computed value is 0.60. A discrepancy amounting to a factor of 10 between the observed and expected intensities has to be attributed to the blending of some unidentified strong lines. The observed line at 1009.7 Å is probably a blend of C II and Ne VI lines.

In Table I we have listed the expected and the theoretical intensities for the various Ne VI lines. The expected intensities in column 3 refer to the values derived from the constancy of the relative population of the fine structure levels and the observed intensity of the 562.80 Å line. Theoretical intensities in column 5 have been obtained by assuming: (i) spherically-symmetric model solar atmosphere (Elzner, 1976), (ii) density dependent ionization calculations of Jordan (1969), and (iii) the value of 3.98×10^{-5} for the element abundance of neon (Kato, 1976). We have calculated, in addition, theoretical line intensities using (a) low density ion fractions obtained by Jordan (1969), (b) low density ion fractions published by Arnaud and Rothenflug (1985). In case (a) Mg VI line intensities are 50% more than that of the high density case (Jordan, 1969) and Ne VI line intensities are 15% more than that of the high density case (Jordan, 1969). In case (b) Mg VI line intensities are 40% more than that of the high density case and Ne VI line intensities are 5% less than that of the high density case.

TABLE I

Line intensities of Ne VI lines

Transition $2s2p^2 \rightarrow 2s^22p$	Wavelength[a] (Å)	Intensities (ergs cm^{-2} s^{-1} sr^{-1})		
		Expected[c]	Observed[b]	Computed[c]
$^2D_{5/2} - {}^2P^0_{3/2}$	562.80	16.65		17.81
$^2D_{3/2} - {}^2P^0_{3/2}$	562.71	1.66	18.31 (Ne VI, Ne VII)[c]	1.78
$^2D_{3/2} - {}^2P^0_{1/2}$	558.59	9.40	18.95 (Ne VI, Ca X)[c]	10.04
$^2S_{1/2} - {}^2P^0_{3/2}$	435.65	7.10	28.32 (Ne VI, Mg VII)[c]	7.57 (2.27, 434.71 Å: Mg VII; 13.39, 434.92 Å: Mg VII)
$^2S_{1/2} - {}^2P^0_{1/2}$	433.18	4.26	–	4.54
$^2P_{1/2} - {}^2P^0_{3/2}$	403.26	4.55	25.73 (Ne VI, Mg VI)[c]	4.83
$^2P_{3/2} - {}^2P^0_{3/2}$	401.93	21.96		23.40
$^2P_{1/2} - {}^2P^0_{1/2}$	401.14	8.30	89.00	8.85
$^2P_{3/2} - {}^2P^0_{1/2}$	399.82	4.41	(Mg VI)[c]	4.69
$^4P_{5/2} - {}^2P^0_{3/2}$	999.60	0.92	(Si XII)[c]	1.0
$^4P_{3/2} - {}^2P^0_{3/2}$	1006.1	0.55	5.02 (Ne VI)	0.60
$^4P_{1/2} - {}^2P^0_{3/2}$	1010.6	0.15	11.51 (Ne VI, C II)[c]	0.16

[a] Ne VI (Kelly and Palumbo, 1973), Mg VI (Edlén, 1984).
[b] Vernazza and Reeves (1978).
[c] Cf. text.

Mg VI lines: in the list of observed lines there are only two lines which have been assigned the status of probable identification. These are at 403.31 Å and 399.28 Å. Both these have been discussed along with the Ne VI lines. The line at 400.66 Å has also been discussed along with Ne VI lines. The lines at 388.0 Å ought to be observable with their combined intensities. The observed line at 349.8 Å with an intensity of 133.11 ergs cm^{-2} s^{-1} sr^{-1} may belong to Si IX. The nearby Mg VI lines at 349 Å have sufficient intensity to be observable at high spectral resolution. The Mg VI lines at 314 Å would blend with 313.74 Å of Mg VIII and 314.35 Å line of Si VIII. Vernazza and Reeves list only the Mg VIII lines but no intensity values are given for the quiet areas. No line identified at 293 Å. Mg VI lines at 291.4 Å are close to an observed line at 292.1 Å but its identification with Ni XVIII is uncertain. There is, however, a S XI line at 291.59 Å (not listed by Vernazza and Reeves) with an intensity 6.21 ergs cm^{-2} s^{-1} sr^{-1} (Malinovsky and Héroux, 1973). No intensity value is given for this observed line. The two lines at 270.4 Å are not within the wavelength range considered by Vernazza and Reeves. However, these lines would be blended by a very strong Fe XIV line at 270.51 Å (Malinovsky and Héroux, 1973). We are not aware of any observational information on the line at 268.99 Å. The line at 1190.12 Å would be blended by 1190.40 Å Si II and

1189.6 Å C I lines. We have computed intensities for several Mg VI lines under the same assumption as for the Ne VI lines. We have assumed a value of 3.16×10^{-5} for the Mg element abundance (Kato, 1976). This abundance value seems to be appropriate since it gives rather excellent agreement between computed and expected intensities at 434.6 Å. In Table II we have listed the Mg VI line intensities.

TABLE II

Line intensities of Mg VI lines

Transition $2s2p^4 \rightarrow 2s^22p^3$	Wavelength[a] (Å)	Intensities (ergs cm^{-2} s^{-1} sr^{-1}) Observed[b]	Calculated[c]
$^4P_{5/2} - {}^4S^0_{3/2}$	403.31	25.73 (Ne VI, Mg VI)[c]	13.01
$^4P_{3/2} - {}^4S^0_{3/2}$	400.66	–	8.81
$^4P_{1/2} - {}^4S^0_{3/2}$	399.28	30.06 (Mg VI)[c]	4.53 –
$^2D_{5/2} - {}^2P^0_{3/2}$	388.00	–	1.04
$^2D_{3/2} - {}^2P^0_{3/2}$	387.93	–	0.12
$^2D_{3/2} - {}^2P^0_{1/2}$	387.77	–	0.58
$^2D_{5/2} - {}^2D^0_{3/2}$	349.18	–	0.36
$^2D_{5/2} - {}^2D^0_{5/2}$	349.16	133.11 (Si IX)[c]	6.77
$^2D_{3/2} - {}^2D^0_{3/2}$	349.12	–	5.11
$^2D_{3/2} - {}^2D^0_{5/2}$	349.11	–	0.49
$^2S_{1/2} - {}^2P^0_{3/2}$	314.65	(Mg VIII, Si VIII)[c]	0.93
$^2S_{1/2} - {}^2P^0_{1/2}$	314.54	–	0.53
$^2P_{3/2} - {}^2P^0_{3/2}$	293.11	–	1.26
$^2P_{3/2} - {}^2P^0_{1/2}$	293.02	–	0.28
$^2P_{1/2} - {}^2P^0_{3/2}$	291.46	(Ni XVIII, S XI)[c]	0.53
$^2P_{1/2} - {}^2P^0_{1/2}$	291.36	–	0.53
$^2P_{3/2} - {}^2D^0_{3/2}$	270.40	(Fe XIV)[c]	0.83
$^2P_{3/2} - {}^2D^0_{5/2}$	270.39	–	6.08
$^2P_{1/2} - {}^2D^0_{3/2}$	268.99	–	3.03
$2s^22p^3 \rightarrow 2s^22p^3$			
$^2P_{1/2} - {}^4S^0_{3/2}$	1191.67	–	0.37
$^2P_{3/2} - {}^4S^0_{3/2}$	1190.12	26.41 (Si II, C I)[c]	1.22

[a] Ne VI (Kelly and Palumbo, 1973), Mg VI (Edlén, 1984).
[b] Vernazza and Reeves (1978).
[c] Cf. text.

5. Electron Density and Temperature Diagnostics

Ne VI and Mg VI lines originate predominantly in the chromosphere–corona transition region. The ionization equilibrium curves for Ne VI and Mg VI overlap around the temperature for maximum relative ion abundance. Moreover, the quiet-Sun electron pressure parameter $(n_e T)$ seems to have a constant canonical value of 6×10^{14} cm^{-3} K. We have calculated several line intensity ratios as a function of electron density and temperature and keeping the electron pressure constant. This procedure is meaningful because the observed line intensities refer to the average physical conditions of the emitting layers within which electron densities and temperatures vary but the electron pressure remains constant. Thus we will get the effective electron density and the corresponding temperature from a particular line intensity ratio. We have considered three different cases of line intensity ratios.

5.1. Intensity ratios using Ne VI lines

These ratios are independent of the ionic concentrations and the element abundance. In Figure 1 we have plotted the various ratios against electron density. The corresponding temperature is given by the constant electron pressure parameter. In view of the excellent agreement between the expected and computed intensities we assume the theoretical ratios, for the sake of consistency, to represent the expected ratios. The filled circles in Figure 1 refer to the theoretical ratios. In Table III we have listed some of the ratios and the corresponding derived electron densities and temperatures.

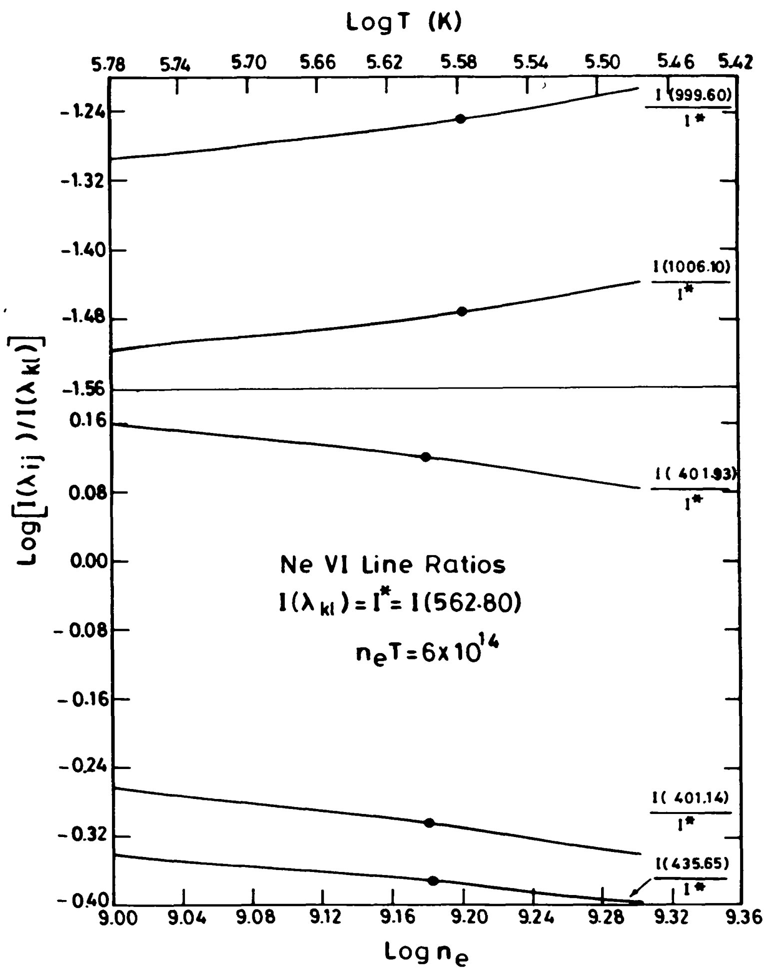

Fig. 1. Log of theoretical intensity ratios $I(\lambda_{ij})/I(\lambda_{kl})$ for Ne VI lines as a function of $\log n_e$ and $\log T$ for a constant electron pressure parameter $n_e T$ (= 6 × 10^{14} cm^{-3} K). The corresponding $\log T$ scale is shown at the top. The filled circles refer to the theoretical intensity ratios. λ_{ij} and λ_{kl} are in Å. Density-dependent ion fractions have been used (Jordan, 1969).

TABLE III

Electron densities and temperatures derived from Ne VI line ratios

$\lambda'(\text{Å})/\lambda(\text{Å})$	$n_e\,(\text{cm}^{-3})$	$T\,(\text{K})$
401.14/562.80	1.51×10^9	3.97×10^5
401.93/562.80	1.51×10^9	3.97×10^5
435.65/562.80	1.52×10^9	3.95×10^5
999.6/562.80	1.59×10^9	3.77×10^5
1006.1/562.80	1.59×10^9	3.77×10^5

We notice that we get different temperatures and electron densities. This is due to the fact that line intensity ratios contain a sensitive exponential factor involving the line wavelengths and the temperature.

5.2. Intensity ratios using Mg VI lines

We have chosen the 314.65 Å line as reference line to obtain intensity ratios for the following reasons. The upper level of the transition for this line is $2s2p^4\,{}^2S_{1/2}$ which is radiatively connected only to the levels $2s^22p^3\,{}^2P_{3/2,\,1/2}$. The ${}^2P_{3/2,\,1/2}$ levels show relatively more sensitivity to electron density variations than the other fine structure levels of the ground term. We have combined the intensities of three lines at 388 Å for estimating the ratio. Similarly four lines at 349 Å have been combined into one line. In Figure 2 we have plotted the various ratios against electron density. The corresponding temperature is given by the electron pressure parameter. In view of the excellent agreement between some of the computed and expected Ne VI line intensities with the help of Mg VI and Mg VII line intensities, we assume, for the sake of consistency, theoretical Mg VI line intensities to represent the expected Mg VI line intensities. The filled circles in Figure 2 represent the theoretical ratios. The derived electron densities and temperatures from the various line ratios are given in Table IV.

As in the case of Ne VI different ratios give different electron density and temperature values. The Mg VI ion has maximum ionic abundance at 3.76×10^5 K, same as Ne VI. The temperatures derived from Mg VI line ratios are larger because the layers contributing to the observed line intensities are relatively broader for temperatures greater than the temperature for maximum ion concentration than is the case for Ne VI lines. For temperatures less than the temperature for maximum ion concentration the layers contributing to Mg VI lines are thinner than those for Ne VI lines.

5.3. Intensity ratios using Ne VI lines and the resonance line of Mg VI

In Figures 3 and 4 we have shown the Ne VI to Mg VI line intensity ratios as a function of electron density and temperature. We have chosen the resonance line at 400.66 Å as the reference line. The various intensity ratios and the derived electron densities and temperatures are given in Table V.

In this case the line intensity ratios are dependent, in addition, on the relative element abundances and the relative ionic concentrations of Ne VI and Mg VI. The intensity ratio

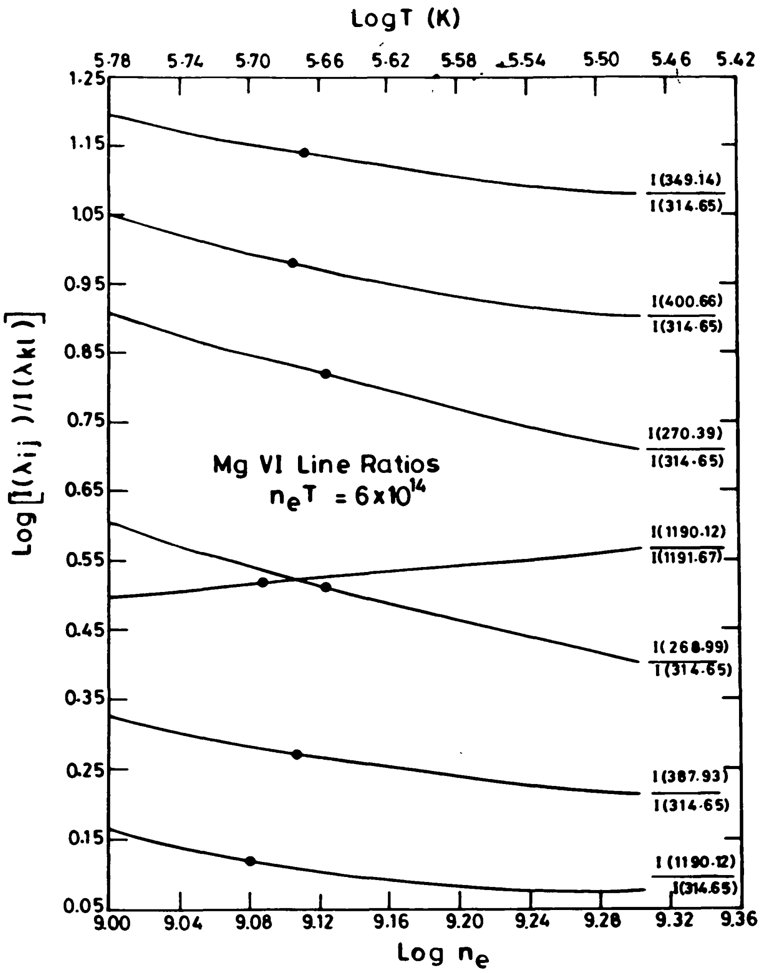

Fig. 2. Same as Figure 1 but for Mg VI lines.

TABLE IV

Electron densities and temperatures derived from Mg VI line ratios

λ'(Å)/λ(Å)	n_e (cm^{-3})	T (K)
268.99/314.65	1.33×10^9	4.51×10^5
270.39/314.65	1.33×10^9	4.51×10^5
349.14/314.65	1.29×10^9	4.65×10^5
387.93/314.65	1.28×10^9	4.69×10^5
400.66/314.65	1.27×10^9	4.72×10^5
1190.12/314.65	1.20×10^9	5.00×10^5
1190.12/1191.67	1.22×10^9	4.92×10^5

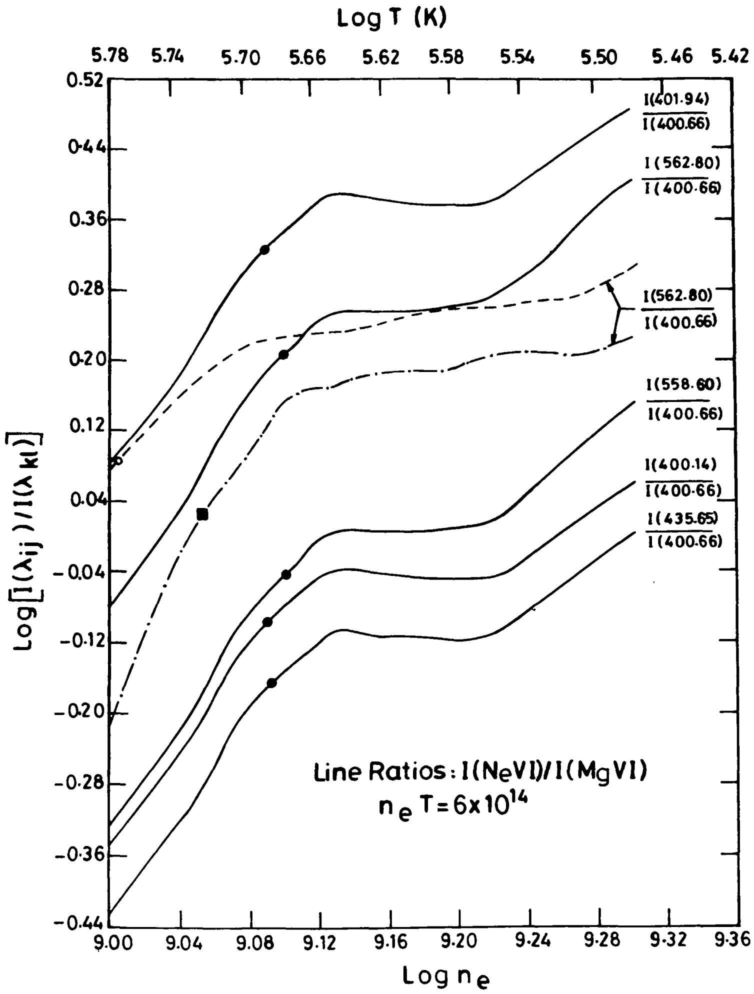

Fig. 3. Same as Figure 1 but for Ne VI lines with respect to the 400.66 Å Mg VI line. ----: theoretical curve using low density ion fractions given by Jordan (1969). —·—·—·: theoretical curve using low density ion fractions published by Arnaud and Rothenflug (1985). Open circle and filled square represent theoretical ratios.

TABLE V

Electron densities and temperatures derived from Ne VI/Mg VI line ratios

λ'(Å)/λ(Å)	n_e (cm^{-3})	T (K)
401.14/400.66	1.23×10^9	4.88×10^5
401.94/400.66	1.23×10^9	4.88×10^5
435.65/400.66	1.24×10^9	4.84×10^5
558.65/400.66	1.26×10^9	4.76×10^5
562.80/400.66	1.26×10^9	4.76×10^5
999.6/400.66	1.29×10^9	4.65×10^5
1006.1/400.66	1.29×10^9	4.65×10^5

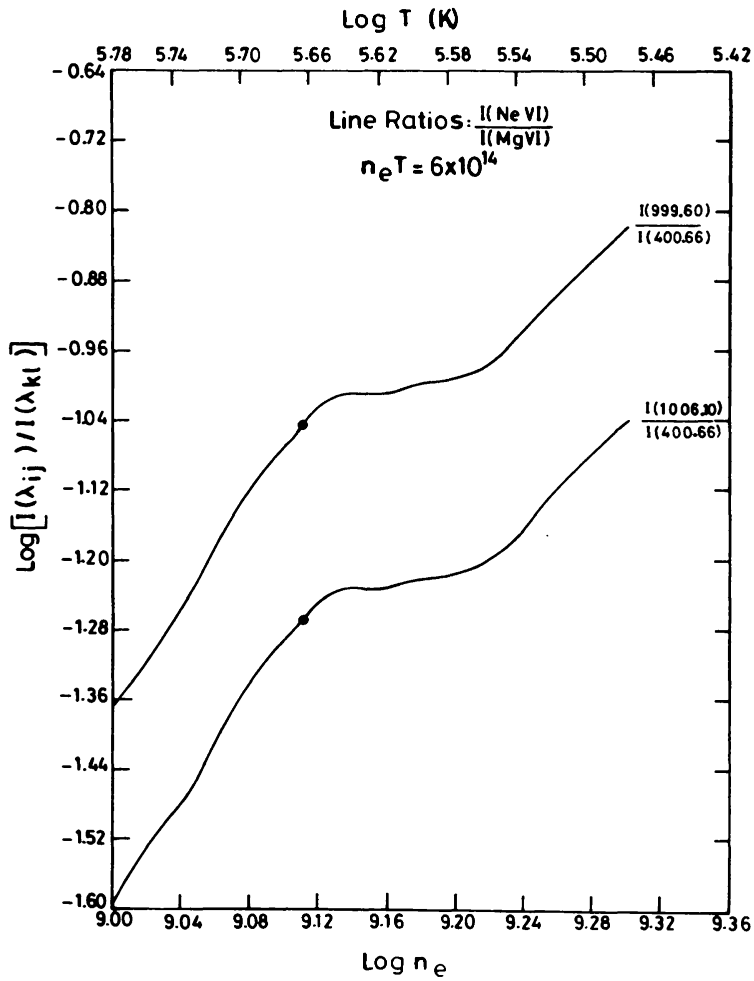

Fig. 4. Same as Figure 1 but for Ne VI lines with respect to the 400.66 Å Mg VI line.

curves in Figures 3 and 4 are drawn for equal element abundances of Ne and Mg. The theoretical ratios shown on the curves are the normalised values given by the equation

$$\log\left\{\frac{I(\lambda(\mathrm{Ne\,VI}))}{I(\lambda(\mathrm{Mg\,VI}))}\right\}^{\mathrm{normalized}} = \log\left\{\frac{I(\lambda(\mathrm{Ne\,VI}))}{I(\lambda(\mathrm{Mg\,VI}))}\right\}^{\mathrm{actual}} - \log\left\{\frac{N(\mathrm{Ne})}{N(\mathrm{H})}\bigg/\frac{N(\mathrm{Mg})}{N(\mathrm{H})}\right\}.$$

We have assumed $N(\mathrm{Ne})/N(\mathrm{H}) = 3.98 \times 10^{-5}$ and $N(\mathrm{Mg})/N(\mathrm{H}) = 3.16 \times 10^{-5}$ for the respective element abundances as these values explain the expected line intensities rather well. We notice that the derived electron densities and temperatures are nearly the same as those derived from Mg VI line ratios. This is primarily due to the fact that higher Ne element abundance relative to Mg outweighs the thinness of layers, which contribute to Ne VI lines, at temperatures greater than the temperature for maximum ion concentration.

6. Results and Discussion

The emission coefficient of a line is directly proportional to the number density of the upper level of the transition. Any variation in line emissivity with electron density and temperature would be due to the changes in the population of the upper level. In the present study, the occupation of higher levels is essentially governed by occupation of the ground term levels. Therefore, a change in the occupation of the ground levels would be reflected in the variation in the line emission.

The Ne VI ion has two fine structure levels in the ground state. Since we are concerned here with the averaged quiet-Sun conditions for the chromosphere–corona transition region the relative population of the ground term fine structure levels are rather insensitive to electron density and temperature. Thus, the variation of line ratios shown in Figure 1 are due to the temperature in an exponential form which appears in the line ratios. It can be shown that the line ratio is directly proportional to this exponential factor. It is of the form

$$\exp\left\{-\frac{1.44\times 10^{8}}{T}\left(\frac{1}{\lambda_{ij}(\text{Å})}-\frac{1}{\lambda_{kl}(\text{Å})}\right)\right\}$$

when we express line emissivities in terms of branching ratios and other atomic parameters.

Vernazza and Mason (1978) have considered four Ne VI line ratios. Two of them are common to our ratios. They have considered these ratios at constant temperature. We have considered some additional ratios which have not been discussed by them. Our discussion of Ne VI line ratios at constant pressure seem more appropriate for conditions within the chromosphere–corona transition region. In addition, our discussion of Ne VI lines is more detailed in the light of the observed values listed by Vernazza and Reeves. Moreover, Vernazza and Mason (1978) have scaled the atomic data in an arbitrary manner to fit some observed ratios. This aspect was discussed in detail by Dwivedi and Raju (1980). The comments by Dwivedi and Raju (1980) were later justified in a paper by Brown *et al.* (1986). Very recently Dwivedi and Gupta (1991) have considered Ne VI line ratios. As stated earlier our analysis of observational data on Ne VI lines is more exhaustive.

The Mg VI ion has five fine structure levels in the ground state. This ion has been considered earlier by Feldman *et al.* (1978), Bhatia and Mason (1980), and Raju and Dwivedi (1990). In the present investigation we have used improved atomic data for Mg VI transitions and the line ratios have been discussed, as in the case of Ne VI, at constant electron pressure. Mg VI fine-structure levels are sensitive to electron density values relevant to the chromosphere-corona transition region. Therefore, Mg VI line ratios are useful for electron density and temperature diagnostics of the transition region.

Figures 3 and 4 show the variation of Ne VI to Mg VI line ratio with electron density and temperature at constant electron pressure parameter. These ratios are more sensitive to electron density and temperature than Ne VI or Mg VI line ratios. This is due to the dependence, in addition, of these line ratios on the relative ionic concentrations of

Ne VI and Mg VI. We have used the density-dependent ion fractions computed by Jordan (1969). At high temperatures ionic concentrations of Mg VI is greater than that of Ne VI. This difference decreases with decreasing temperature. This explains the steeper rise of the ratio with increasing electron density. Then a nearly narrow plateau region is reached. This region extends till about the temperature for maximum ionic concentration. Thereafter, the ionic concentration of Mg VI starts decreasing relative to that of Ne VI and the line ratios start increasing with electron density once again. The theoretical ratios are reasonably away from the plateau region and are thus useful for electron density and temperature determinations. We have shown in Figure 3, for the sake of comparison, the theoretical curve for the line ratio $I(562.80)/I(400.66)$ using (a) low-density ion fractions given by Jordan (1969), and (b) low-density ion fractions published by Arnaud and Rothenflug (1985).

The comparison of theoretical and expected intensities of Ne VI and Mg VI lines suggest the need to observe these lines in future at higher spectral resolutions. This will help in resolving the difficulties associated with blending of two or more lines. In particular, lines around 558, 435, 401, 399.8, 349, and 314 Å. The agreement between the theoretical and the available observed Ne VI and Mg VI line intensities is a testimony to the reliability of atomic data, element abundance values of Ne and Mg, and the atmospheric model used in the present study. In literature we find that, depending upon the solar feature being considered, the relative abundance value of neon to magnesium ranges from 0.97 to 3 (Widing, Feldman, and Bhatia, 1986; Widing and Feldman, 1989; Feldman and Widing, 1990). In an extensive review paper Feldman (1992) has shown that element abundances of the upper solar atmosphere are not fixed. It has been emphasized that one must consider the element abundances of the region while calculating the plasma properties of the solar atmosphere. However, our analysis of the ATM data (Vernazza and Reeves, 1978) shows that the value of 1.26 for the relative abundance of neon to magnesium seem to explain the expected intensities for the averaged quiet solar conditions at solar minimum within the chromosphere–corona transition region.

7. Conclusion

We have shown that the assumption of constant electron pressure to estimate electron densities and temperatures within the chromosphere–corona transition region from Ne VI/Mg VI line ratios is a reasonable one. We find that the values of 3.98×10^{-5} and 3.16×10^{-5} for neon and magnesium element abundances respectively seem to give rather good agreement between theoretical and expected intensities based on ATM ultraviolet spectrometer data. This amounts to a value of 1.26 for the ratio of neon to magnesium element abundance for the average quiet-Sun conditions near solar minimum. As has been discussed above the element abundances are not fixed but vary from region to region. Our analysis of the observed Ne VI and Mg VI line intensities for the averaged quiet-Sun conditions suggests the need for future observations at higher spectral resolutions to facilitate more detailed electron density and temperature diagnostics of the chromosphere–corona transition region and derivation of reliable relative abundance of neon to magnesium.

Acknowledgements

One of us (Asheesh K. Gupta) would like to express his gratitude to Professor J. C. Bhattacharyya, Director, Indian Institute of Astrophysics, for the kind hospitality, during the summer of 1990, at the Indian Institute of Astrophysics, Bangalore. The authors are grateful to the unknown referee for valuable comments and suggestions which have helped considerably in improving the presentation.

References

Arnaud, M. and Rothenflug, R.: 1985, *Astron. Astrophys. Suppl.* **60**, 425.
Bhatia, A. K. and Kastner, S. O.: 1988, *Astrophys. J.* **332**, 1063.
Bhatia, A. K. and Mason, H. E.: 1980, *Monthly Notices Roy. Astron. Soc.* **190**, 925.
Brown, W. A., Bruner, M. E., Action, L. W., and Mason, H. E.: 1986, *Astrophys. J.* **301**, 981.
Czyzak, S. J., Aller, L. H., and Euwema, R. N.: 1974, *Astrophys. J. Suppl.* **28**, 465.
Doschek, G. A.: 1984, *Astrophys. J.* **279**, 446.
Dufton, P. L., Doyle, J. G., and Kingston, A. E.: 1979, *Astron. Astrophys.* **78**, 318.
Dwivedi, B. N.: 1988, *Adv. Space Res.* **8**, No. 11, 185.
Dwivedi, B. N. and Gupta, A. K.: 1991, *Adv. Space Res.* **11**, No. 1, 307.
Dwivedi, B. N. and Raju, P. K.: 1980, *Solar Phys.* **68**, 111.
Edlen, B.: 1984, *Phys. Scripta* **30**, 135.
Elzner, L. R.: 1976, *Astron. Astrophys.* **47**, 9.
Feldman, U., Doschek, G. A., Mariska, J. T., Bhatia, A. K., and Mason, H. E.: 1978, *Astrophys. J.* **226**, 674.
Feldman, U. and Widing, K. G.: 1990, *Astrophys. J.* **363**, 292.
Feldman, U.: 1992, *Phys. Scripta* **46**, 202.
Flower, D. R. and Nussbaumer, H.: 1975a, *Astron. Astrophys.* **45**, 145.
Flower, D. R. and Nussbaumer, H.: 1975b, *Astron. Astrophys.* **45**, 349.
Gabriel, A. H. and Jordan, C.: 1972, in E. McDaniel and M. C. McDowel (eds.), *Case Studies in Atomic Collision Physics*, Vol. II, North-Holland Publ. Co., Amsterdam, p. 210.
Giles, K.: 1981, *Monthly Notices Roy. Astron. Soc.* **195**, 63P.
Jordan, C.: 1969, *Monthly Notices Roy. Astron. Soc.* **142**, 501.
Kato, T.: 1976, *Astrophys. J. Suppl.* **30**, 397.
Kelly, R. L. and Palumbo, L. J.: 1973, *Atomic and Ionic Emission Lines below 2000 Å*, NRL Report 7599.
Malinovsky, M. and Héroux, L.: 1973, *Astrophys. J.* **181**, 1009.
Raju, P. K. and Dwivedi, B. N.: 1979, *Pramana* **13**, 319.
Raju, P. K. and Dwivedi, B. N.: 1990, *Astrophys. Space Sci.* **173**, 13.
Saraph, H. E., Seaton, M. J., and Shemming, J.: 1968, *Phil. Trans. Roy. Soc. London* **264**, 77.
Vernazza, J. E. and Mason, H. E.: 1978, *Astrophys. J.* **226**, 720.
Vernazza, J. E. and Reeves, E. M.: 1978, *Astrophys. J. Suppl.* **37**, 485.
Widing, K. G. and Feldman, U.: 1989, *Astrophys. J.* **344**, 1046.
Widing, K. G., Feldman, U., and Bhatia, A. K.: 1986, *Astrophys. J.* **308**, 982.
Wiese, W. L., Smith, M. W., and Miles, B. M.: 1969, *Atomic Transition Probabilities*, Vol. 2, Sodium through Calcium, US Dept. of Commerce, Nat. Bur. Standards.
Zeippen, C. J.: 1982, *Monthly Notices Roy. Astron. Soc.* **198**, 111.